



Understanding the complicated crystallization behaviors in Germanium-Tellurides



Yimin Chen^{a,b,*}, Rongping Wang^{b,**}, Xiang Shen^b, Junqiang Wang^c, Tiefeng Xu^b

^a Department of Microelectronic Science and Engineering, School of Physical Science and Technology, Ningbo University, Ningbo 315211, China

^b Laboratory of Infrared Material and Devices & Key Laboratory of Photoelectric Materials and Devices of Zhejiang Province, Advanced Technology Research Institute, Ningbo University, Ningbo 315211, China

^c CAS Key Laboratory of Magnetic Materials and Devices & Zhejiang Province Key Laboratory of Magnetic Materials and Application Technology, Ningbo Institute of Materials Technology & Engineering, Chinese Academy of Sciences, Ningbo 315201, China

ARTICLE INFO

Keywords:

Germanium-Tellurides
Crystallization behaviors
Singularities
Amorphous structures

ABSTRACT

Crystallization behaviors and configurations of germanium-tellurides ($\text{Ge}_x\text{Te}_{100-x}$) at a wide compositional range ($12.5 \leq x \leq 85$) have been investigated. It is found $\text{Ge}_x\text{Te}_{100-x}$ film exhibits one- or two-step crystallization behavior with a complicated competition between GeTe and Te (or Ge) phases. The composition dependences of crystallization temperature and activation energy have been revealed. They exhibit four singularities at $x = 20.4$ (GeTe_4), $x = 33$ (GeTe_2), $x = 49$ (GeTe), and $x = 22$ ($\text{Ge}_{22}\text{Te}_{78}$). Based on the method of X-ray photoelectron spectroscopy, the structural sketches for the $\text{Ge}_x\text{Te}_{100-x}$ glasses that is helpful to understand the evolution of crystallization behavior are built up. It is evident that, the presence of homopolar Te–Te and heteropolar Ge–Te bonds is the main reason for the structural and thermal stability of Ge-deficient films, and Ge–Ge bond in GeGe_4 tetrahedron appears when $x > 50$ and effectively enhances the stability of Ge-rich films.

1. Introduction

Chalcogenide bulk glasses and thin films have received considerable attention due to their excellent transmission in the infrared and the profound structural transformations upon external energy input like light, thermal and ion irradiation. These excellent properties have opened new technique applications in many areas [1]. For example, Te-based thin films, especially GeTe and GeTe_4 , have been frequently employed in the fields of information storage and optical waveguide in the infrared [2,3]. Ge–Te was first used as one of the phase-change materials in 1986 [4]. By measuring the optical transmission of the sample, the maximum and minimum crystallization temperature were detected at GeTe_4 and GeTe, respectively [4]. It was subsequently reported that, the GeTe_2 film shows the highest crystallization temperature and activation energy in Te-rich system [5]. In Ge-rich film, it was found that, the crystallization temperature increases from 180 °C to 360 °C with increasing Ge content from $\text{Ge}_{50}\text{Te}_{50}$ to $\text{Ge}_{76}\text{Te}_{24}$ [6], and phase separation of Ge and rhombohedral GeTe appears in crystalline Ge-rich films [7]. In the study of Ge-Te films with Ge content from 6 to 54 at%, two-stage crystallization or phase separation was reported in all

the films except GeTe [5]. Other investigations also confirmed that the glasses containing 10 and 15 at% Ge show two-stage crystallization [8,9]. Nevertheless, it was also reported that, the Ge–Te films containing Ge content of 20 and 25 at% exhibit only one-step crystallization with simultaneous formation of GeTe and Te phases [8]. It was also shown that, $\text{Ge}_{30}\text{Te}_{70}$ film crystallizes in a one-step process but $\text{Ge}_{40}\text{Te}_{60}$ film crystallizes in two-step process [10]. These contradicted results are somehow confusing to understand crystallization behavior for Ge-Te system that thus need to be further clarified.

The complicated thermal and crystallization behaviors have aroused the interests in unravelling Ge–Te glass structure. A model including Ge–Te tetrahedra and Te–Te chain has been used to simulate the structural factors of $\text{Ge}_{15}\text{Te}_{85}$ and $\text{Ge}_{20}\text{Te}_{80}$ from high-energy synchrotron X-ray diffraction experiments [11]. Using the reverse Monte-Carlo simulations based on the electron diffraction data, it was shown that large amounts of Te atoms do not bond with Ge in non-stoichiometric Te-rich films [12]. It was also found that, GeTe or GeTe_2 structural units with a random bonding structure exist in amorphous Ge–Te network [13].

Obviously, these models cannot be used to describe the structures of

* Corresponding author at: Department of Microelectronic Science and Engineering, School of Physical Science and Technology, Ningbo University, Ningbo 315211, China.

** Corresponding author.

E-mail addresses: chenyimin@nbu.edu.cn (Y. Chen), wangrongping@nbu.edu.cn (R. Wang).

GeTe and Ge-rich film due to the deficiency of Te. Other models, like the random cubic symmetry distribution [14], ring structure model [15], and ABAB square model [16], were proposed to explain the fast crystallization kinetics of GeTe. Apparently, the so called “8-N” bonding rule was broken in these models. In terms of the mean coordination number (MCN) of Ge and Te, it was found that, they could be Ge(4)-Te(2) (the MCN is 4 and 2 for Ge and Te, respectively) or Ge(3)-Te(3) in Te-rich Ge-Te compounds [17]. Phillips predicated that, in the glass-forming region (Ge content in the range of 10–33 at%), Ge and Te has an MCN of 4 and 2, while for Ge content more than 33 at%, they become 6 and 3, respectively [18]. The MCN of Te and Ge was also reported to be slightly larger than 2 [19–21], and close to 4 in Te-rich film [22], respectively. Although the structural model and MCN of amorphous Ge–Te are discussed intensively in recent years, the evolution of the MCN with varied compositions in the Ge–Te films is unclear yet.

In this work, therefore, we studied the thermal behavior and structures of $\text{Ge}_x\text{Te}_{100-x}$ film at a wide compositional range of $12.5 \leq x \leq 85$. We investigated the crystallization behaviors of the films, and observed four singularities in activation energy and crystallization temperature for the first time. Based on X-ray photoelectron spectroscopy analysis, we proposed structural sketches of the amorphous $\text{Ge}_x\text{Te}_{100-x}$ films to illustrate the complicated crystallization behaviors.

2. Experimental methods

A series of amorphous $\text{Ge}_x\text{Te}_{100-x}$ ($12.5 \leq x \leq 85$) films were deposited on $\text{SiO}_2/\text{Si}(100)$ by the magnetron co-sputtering method using separated Ge and Te target. The base and working pressures were set to $\sim 4 \times 10^{-4}$ and 0.35 Pa, respectively, for each deposition. The thickness was *in-situ* controlled by a thickness monitor equipped in the vacuum chamber and *ex-situ* checked by Veeco Dektak 150 surface profiler in air. The film thickness is in a range of 1.2–1.6 μm for $\text{Ge}_x\text{Te}_{100-x}$ films. The thickness fluctuation is less than 2%. The compositions of the films are examined by the Energy Dispersive X-ray Spectroscopy (EDS) more than 5 times in the different position, and the results are listed in Table 1. The temperature dependent sheet resistance (*R-T*) of the as-deposited film was measured using a homemade system based on the four-probe method in a nitrogen atmosphere. The crystallization behaviors were detected by X-ray diffraction (XRD, Bruker D2) in the 2θ range of 10–60° using Cu K α radiation with a wavelength of 0.154 nm. The bonding structures were examined by X-ray photoelectron spectroscopy (XPS, Scienta ESCA-300 spectrometer) with monochromatic Al

Table 1

The peak temperatures for crystallization (T_{p1} and T_{p2}) and the activation energy for first crystallization (Q) of $\text{Ge}_x\text{Te}_{100-x}$.

Ge (at%)	T_{p1} (K)	T_{p2} (K)	Q (eV)	Ge (at%)	T_{p1} (K)	T_{p2} (K)	Q (eV)
12.5	443.5	504.2	1.62	29	521.6	–	3.50
14.5	446.5	504	1.84	30	525.1	–	3.75
16.0	448	500	1.87	33	526.9	–	4.51
17.0	456.3	502	2.04	36	524	526	4.44
19.2	517	–	2.20	38	520.8	522.9	4.28
19.8	518.2	–	2.98	44	503	512	3.93
20.4	519.5	–	3.11	49	470.4	–	3.67
21.7	519.6	–	2.96	55	505.7	515	3.74
22	464.8	505.5	2.09	66	625	628	3.89
23	501.4	–	2.70	75	632	638	4.60
25	508.7	–	2.88	82	650	652.9	4.99
26	512.8	–	3.13	85	656	–	5.44

K α X-rays of 1486.6 eV and energy step of 0.05 eV. The XPS data analysis was conducted with CasaXPS software package.

3. Results and discussion

Typical *R-T* curves of $\text{Ge}_x\text{Te}_{100-x}$ at different heating rates were shown in the left panel of Fig. 1. The corresponding differential curves which were used to accurately determine the peak temperature for crystallization (T_p) were shown in the middle panel of Fig. 1. The values of T_p at a heating rate of 20 K min^{-1} for various Ge-Te compound were put forward in Table 1. The results can be summarized as follows. When $19.2 \leq x \leq 21.7$, $23 \leq x \leq 33$, $x \approx 50$ and 85, the films show one-step crystallization behavior with only one T_p . In all other cases, they exhibit two-step crystallization behavior with two T_p . Especially in $33 < x < 50$, two T_p s are very close and this has been confirmed by the time-resolved XRD data from Raoux et al. [11]. In amorphous $\text{Ge}_x\text{Te}_{100-x}$, it was reported that the glass transition temperature (T_g) increases as Ge content increased, and it is not detectable when Ge content is more than 31 at% [22]. We found a similar result in this work but the details are not shown here. However, there is a sharp drop of T_g was revealed in $\text{Ge}_{22}\text{Te}_{78}$ film, i.e., the T_g value is 450 and 410 K for $\text{Ge}_{21.7}\text{Te}_{78.3}$ and $\text{Ge}_{22}\text{Te}_{78}$, respectively. We believe the sharp drop of T_g is due to the collapsed thermal stability in $\text{Ge}_{22}\text{Te}_{78}$ film.

The XRD method was used to detect the crystalline phases in Ge-Te films. As shown in the bottom of Fig. 2(a)–(g), the red lines represent the standard diffraction peaks that belong to crystalline GeTe phase (PDF No. 7-125), the blue lines correspond to the crystalline Te phase (PDF No. 1-727) and the olive lines to crystalline Ge (PDF No. 3-478). It can be seen that, with increasing annealing temperature, Te phase is precipitated out first, and then GeTe crystalline phase begins to present in $\text{Ge}_{17}\text{Te}_{83}$ and $\text{Ge}_{22}\text{Te}_{78}$ as shown in Fig. 2(a) and (c), respectively. However, these two crystalline phases appear simultaneously with increasing annealing temperature in $\text{Ge}_{20}\text{Te}_{80}$ and $\text{Ge}_{25}\text{Te}_{75}$ as shown in Fig. 2(b) and (d), respectively. It is obvious that, GeTe crystallizes ahead of crystallized Te in $\text{Ge}_{38}\text{Te}_{62}$ with increasing annealing temperature as shown in Fig. 2(e). Such crystallized Te phase is completely suppressed in Fig. 2(f) where only crystallized GeTe is precipitated. In Fig. 2 (g) corresponding to $\text{Ge}_{85}\text{Te}_{15}$ film, both GeTe and Ge crystalline phases are found in the film annealed at 450 °C.

The one- or two-step crystallization behaviors found in the XRD patterns are in agreement with those in Fig. 1 for $\text{Ge}_x\text{Te}_{100-x}$ films ($12.5 \leq x \leq 85$). Interestingly, GeTe is crystallized after crystalline Te phase appears in $\text{Ge}_{22}\text{Te}_{78}$, while GeTe is crystallized first and then Te phase in $\text{Ge}_x\text{Te}_{100-x}$ films when $33 < x < 50$, and GeTe is crystallized before Ge phase in $\text{Ge}_x\text{Te}_{100-x}$ films when $50 < x < 85$. Moreover, four singularities include two maxima and two minima in compositional dependent T_p for the first crystallization process can be detected, i.e., $\text{Ge}_{20.4}\text{Te}_{79.6}$ (GeTe_4), $\text{Ge}_{33}\text{Te}_{67}$ (GeTe_2), $\text{Ge}_{49}\text{Te}_{51}$ (GeTe), and peculiar $\text{Ge}_{22}\text{Te}_{78}$. The maximum T_p s around GeTe_4 and GeTe_2 have been carried out by the previous researches [4,5]. The stoichiometric GeTe is well known as phase-change material due to its fastest crystallization speed with a relative lower T_p in Ge-Te system. Interestingly, the minimum T_p in the peculiar component of $\text{Ge}_{22}\text{Te}_{78}$ which also exhibits phase separation behavior has never been revealed before. It should be emphasized that, the results of conventional differential scanning calorimetry from our previous work is in excellent agreement with the results shown in Fig. 1. Together with the results from XRD, we plotted phase diagram of crystallization for $\text{Ge}_x\text{Te}_{100-x}$ films as shown in Fig. 3, to understand the complicated crystallization behaviors in binary Germanium-Telluride materials.

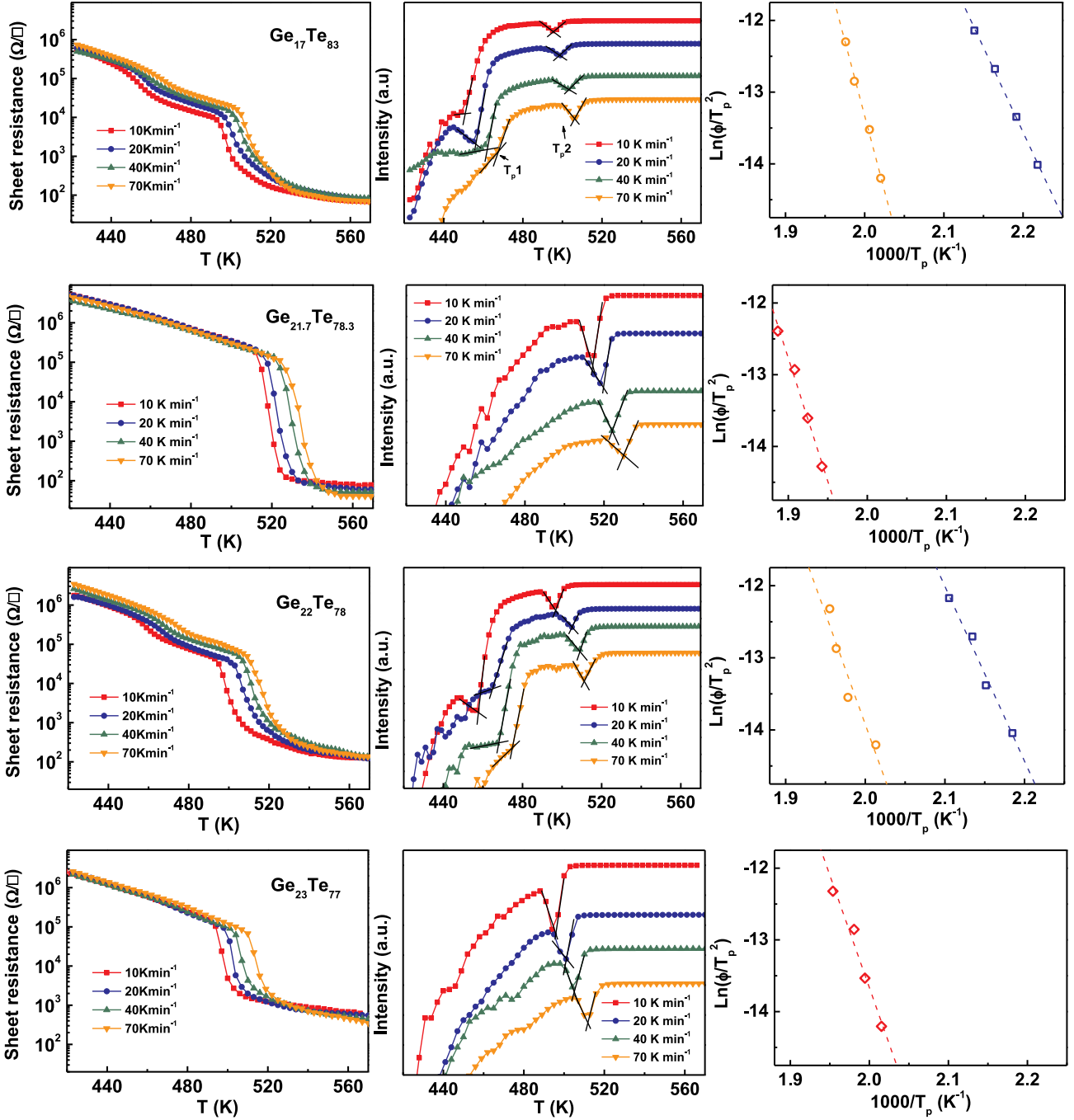


Fig. 1. The R - T curves at different heating rates (left panel), i.e., 10, 20, 40, and 70 K min^{-1} , for $\text{Ge}_{17}\text{Te}_{83}$, $\text{Ge}_{21.7}\text{Te}_{78.3}$, $\text{Ge}_{22}\text{Te}_{78}$, and $\text{Ge}_{23}\text{Te}_{77}$, respectively. The corresponding differential curves and Kissinger plots are shown in middle and right panel, respectively.

The activation energy for crystallization (Q) was calculated by the Kissinger method [24]:

$$\ln(\phi/T_p^2) = -Q/RT_p + A$$

where ϕ is the heating rate, T_p is the peak temperature for

crystallization at a given heating rate, R is the gas constant, and A is a constant. The Kissinger plots of these films are shown in the right panel of Fig. 1. The calculated values of Q for the first crystallization of $\text{Ge}_x\text{Te}_{100-x}$ were listed in Table 1, and the composition dependence of Q was plotted and shown in Fig. 4. Two maxima and two minima of Q can be found in $\text{Ge}_{20.4}\text{Te}_{79.6}$ (GeTe_4), $\text{Ge}_{33}\text{Te}_{67}$ (GeTe_2), $\text{Ge}_{49}\text{Te}_{51}$ (GeTe),

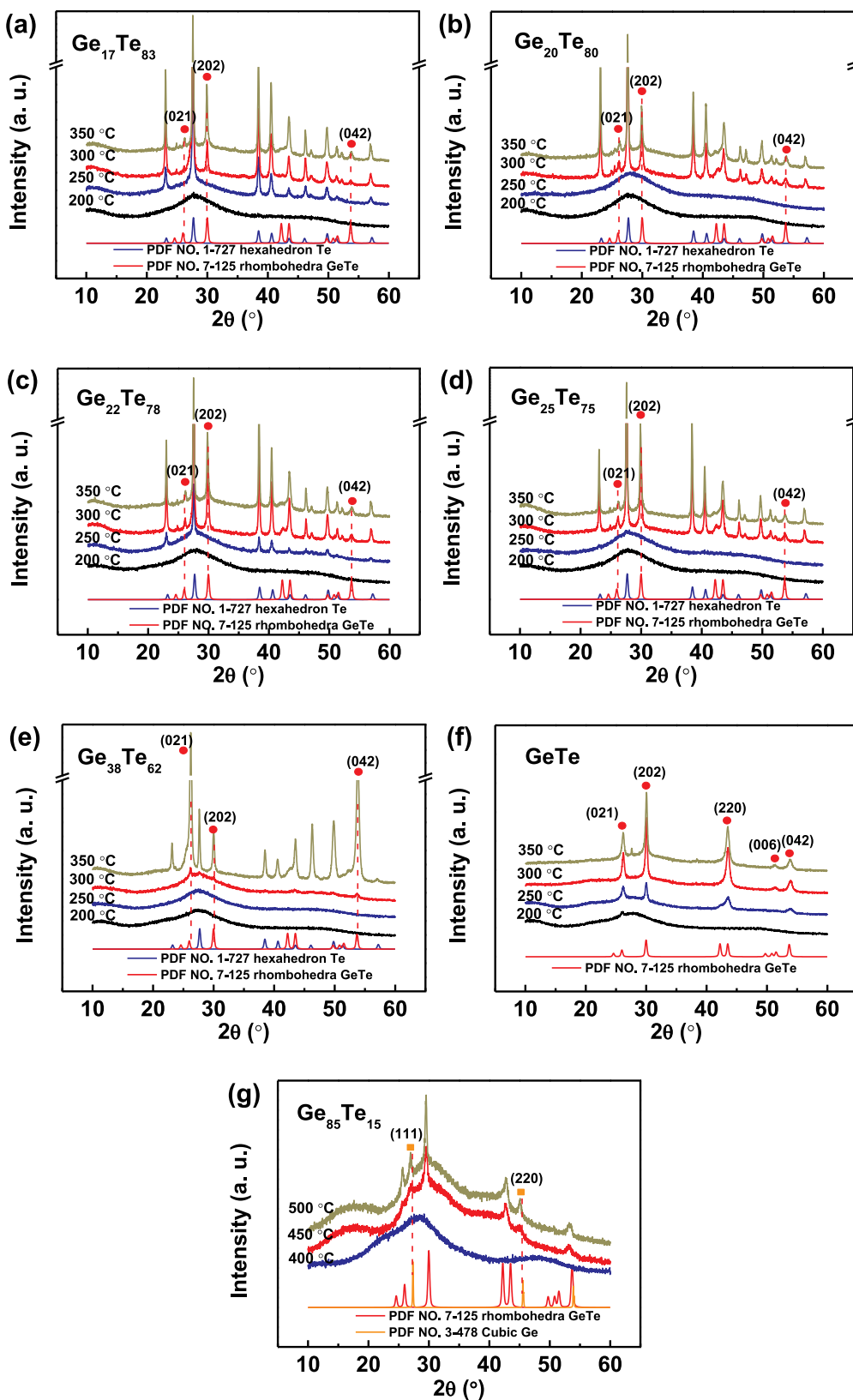


Fig. 2. XRD curves for different temperature annealed Ge_xTe_{100-x} film in composition of (a) Ge₁₇Te₈₃, (b) Ge₂₀Te₈₀, (c) Ge₂₂Te₇₈, (d) Ge₂₅Te₇₅, (e) Ge₃₈Te₆₂, (f) Ge₅₀Te₅₀, and (g) Ge₈₅Te₁₅. The annealing temperatures are 200, 250, 300, and 350 °C for Te-rich Ge-Te and Ge₅₀Te₅₀ film, but they are 400, 450, and 500 °C for Ge₈₅Te₁₅ film. Three XRD curves represent crystalline Te (blue), GeTe (red) and Ge (yellow) from standard PDF cards are listed in the patterns to figure out the crystalline compounds in these films. Red dots and yellow squares indicate the crystalline GeTe and Ge phase in the films. (For interpretation of the references to color in this figure legend, the reader is referred to the web version of this article.)

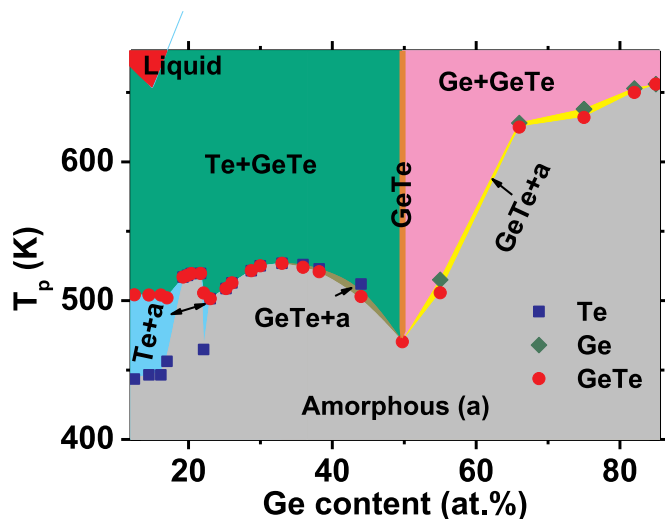


Fig. 3. Phase diagram of crystallization for $\text{Ge}_x\text{Te}_{100-x}$ films. Blue squares, olive diamonds, and red dots represent the crystalline Te, Ge, and GeTe phases, respectively. The shadows with different colors indicate the different state of Ge–Te. The red shadow located at top left corner in the figure represents the liquid Ge–Te, which is ascribed to the low melting temperature in Te-rich eutectic alloys [23]. (For interpretation of the references to color in this figure legend, the reader is referred to the web version of this article.)

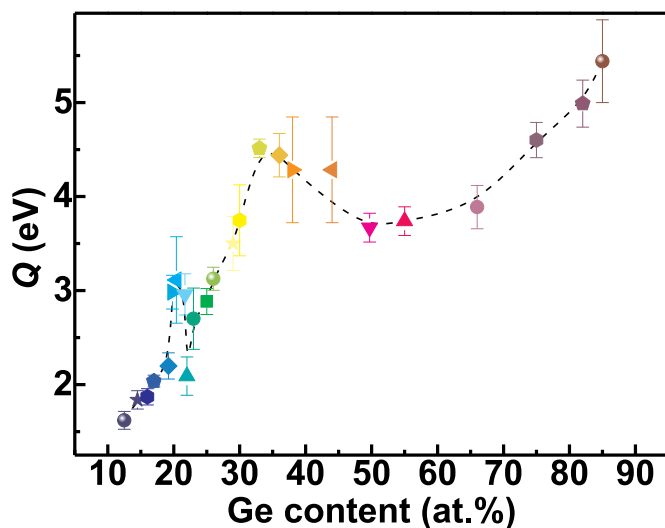


Fig. 4. Component dependent activation energy (Q) for the first crystallization of Ge–Te system. The differently colored data points represent the Q value for different Ge–Te film. Dashed line through the data points is only a guide to the eye.

and $\text{Ge}_{22}\text{Te}_{78}$, respectively. The variation trend of Q is in good agreement with that of T_{p1} in Fig. 2. The results of maximum around GeTe_2 and the minimum at GeTe are in line with other reports [5]. The maximum around GeTe_4 is presented rarely. Nevertheless, the component of $\text{Ge}_{22}\text{Te}_{78}$, which shows a collapse in activation energy for crystallization, has not been reported yet.

The structural evolution with distinct chemical bond in different component that results the complicated crystallization behaviors in

simple binary Ge–Te system was examined by XPS method. Ge and Te 3d spectra of typical Ge–Te films were recorded. The compositions of these Ge–Te films were calculated by integrating the XPS spectra. It results a negligible difference in Ge content (< 0.5 at%) compared to those from EDS tests, and confirms the reliability of the compositions in this work. The adsorbed hydrocarbon was used as the internal reference and the binding energies of C 1s line was referenced at 284.5 eV. We decomposed the Te 3d spectrum into doublets by removing the Shirley baseline. The doublet separation was fixed and then the spectra were fitted with good fitting quality, the results were shown in Fig. 5(a). According to such Te 3d spectra, the content of Ge–Te and Te–Te bond can be extrapolated. Fig. 5(b) is the composition dependent normalized content of Ge–Te and Te–Te bond. An abrupt change can be found when the Ge content close to 22 at%, indicating an obvious change of the structure in Ge–Te films.

Previous investigations showed that, unlike chalcogen elements S and Se that always has an almost fixed mean coordination number of 2, the MCN of Ge could change from 4 to 3 and that of Te could change from 2 to 3 in $\text{Ge}_x\text{Te}_{100-x}$ with increasing Ge content. Following this and XPS results, we constructed a compositional dependent structural sketch for amorphous Ge–Te system as shown in Fig. 6(a). Compositional dependent ratios of the different bonds in those structural sketches were exhibited in Fig. 6(b). It is evidenced that, the ratio of Te–Te bond exhibits a minimum at $\text{Ge}_{20}\text{Te}_{80}$ ($\text{Ge}_3\text{Te}_{12}$) and $\text{Ge}_{33}\text{Te}_{67}$ ($\text{Ge}_6\text{Te}_{12}$), respectively, and an abrupt increase at $\text{Ge}_{22}\text{Te}_{78}$ ($\text{Ge}_4\text{Te}_{14}$). On the contrary, the ratio of Ge–Te bond shows a maximum at $\text{Ge}_3\text{Te}_{12}$ and $\text{Ge}_6\text{Te}_{12}$, respectively, and a sharp decrease in $\text{Ge}_4\text{Te}_{14}$. All these is in good agreement with the results from XPS analyses (see Fig. 5(b)), and thus it presents a plausible explanation of the observed results based on such sketches. In addition, Ge–Ge bond occurs and increases obviously when Ge content is more than 33 and 50 at%, respectively.

In Fig. 6(a), $\text{Ge}_2\text{Te}_{12}$ represents the typical structure in a compositional range of $12.5 \leq x < 19.2$ where Te–Te chain is highlighted as red cycle. In such structure, Te phase crystallizes firstly at relatively low temperature due to the flexible Te–Te chain, and subsequently GeTe phase is separated out at high temperature. $\text{Ge}_3\text{Te}_{12}$ represents the structure in the compositional range of $19.2 \leq x \leq 21.7$, where Te–Te bond is highlighted as blue cycle. Such Te–Te bond is not easy to be precipitated from the network since it is connected to Ge atoms forming stronger Ge–Te bond. It results in a delay of Te phase separation, and therefore, crystalline Te phase would be separated out simultaneously with the formation of GeTe crystalline phase after breaking of Ge–Te bonds, which certainly enhances the thermal stability of the $\text{Ge}_x\text{Te}_{100-x}$ films. However, an isostatic structure in $\text{Ge}_3\text{Te}_{12}$ is collapsed with a slight increase of Ge in the glass network. It causes the Te–Te chain that is highlighted as red cycle presents in Fig. 6(a) again. Thus, the thermal stability is destroyed and it leads to a two-step crystallization behavior where Te phase crystallizes first and GeTe is separated out subsequently.

With further increase of Ge content, the pure Te–Te chain is absent again, and then the structure becomes stable and Te phase is separated out simultaneously with GeTe phase. As illustrated in Fig. 6(a), such configuration and crystallization behavior are presented in $\text{Ge}_4\text{Te}_{12}$ ($\text{Ge}_{25}\text{Te}_{75}$), $\text{Ge}_5\text{Te}_{12}$ ($\text{Ge}_{29}\text{Te}_{73}$), and $\text{Ge}_6\text{Te}_{12}$ ($\text{Ge}_{33}\text{Te}_{67}$). When $x = 33$, GeTe_4 tetrahedron is dominated throughout the whole structure. It results in the second maximum in thermal stability for Ge–Te system. At $x > 33$, such as $\text{Ge}_8\text{Te}_{12}$ ($\text{Ge}_{40}\text{Te}_{60}$) as shown in Fig. 6(a), the structural stability is destroyed by the relative excess Ge. Ge–Te bond is distributed throughout the structure, so the GeTe phase can be easily precipitated.

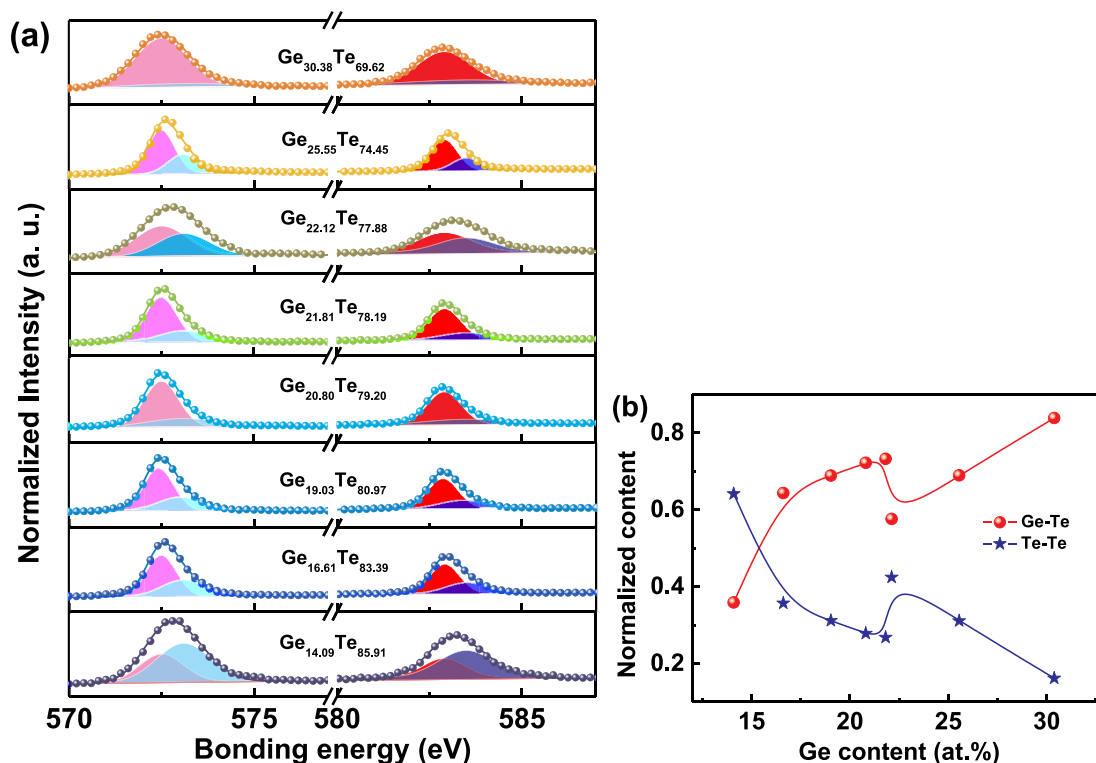


Fig. 5. (a) Te 3d XPS spectra of Ge–Te films. (b) Composition dependence of normalized content for Ge–Te and Te–Te bond.

The atomic configurations of $\text{Ge}_{12}\text{Te}_{12}$ (GeTe) and $\text{Ge}_{15}\text{Te}_{12}$ ($\text{Ge}_{55}\text{Te}_{45}$) are also presented in Fig. 6(a). A number of four-atomic rings that are highlighted by black quadrilaterals exist in amorphous GeTe structure, which is the basic configuration in crystalline GeTe, and they can accelerate the crystallization speed. This has been reported in the ring statistics analogy [15] and *ABAB* square model [16]. The number of Ge-Ge bond increases apparently when $x > 50$, which is in line with other reports [6,25]. As we can see, for Ge-rich Ge–Te ($\text{Ge}_{55}\text{Te}_{45}$) film, the thermal stability is enhanced by the presence of GeGe_4 tetrahedron that is marked as green dashed square in Fig. 6(a). It exhibits two-stage crystallization process with the formation of GeTe phase first and then Ge phase.

4. Conclusions

In this work, the crystallization behaviors and thermal properties of the as-deposited $\text{Ge}_x\text{Te}_{100-x}$ ($12.5 \leq x \leq 85$) film were systematically studied. Based on the methods of *R-T*, XRD, it was found that, $\text{Ge}_x\text{Te}_{100-x}$ exhibits two-step crystallization behavior with the formation of Te phase ahead of GeTe phase at $x < 19.2$, one-step crystallization behavior with simultaneous formation of Te and GeTe phases at $19.2 \leq x \leq 33$ (except $x = 22$), and two-step crystallization behavior with the formation of GeTe phase ahead of Te phase (or Ge phase) at $x > 33$. Only GeTe crystalline phase is precipitated in the stoichiometric GeTe. Moreover, the two-step crystallization behavior with the formation of Te ahead of GeTe phase is also detected in $\text{Ge}_{22}\text{Te}_{78}$. Two maxima and two minima of compositional dependent crystallization temperature and activation energy for the first crystallization have been obtained, which is located at $x = 20.4$ (GeTe_4), $x = 33$ (GeTe_2), $x = 49$ (GeTe), and $x = 22$ ($\text{Ge}_{22}\text{Te}_{78}$), respectively. The peculiar

crystallization behavior of $\text{Ge}_{22}\text{Te}_{78}$ results in a collapse in the thermal stability. Moreover, from the results of XPS spectra and the previous studies about the coordination number of Ge and Te, a plausible sketch of structural evolution has been proposed in this work for better understanding the compositional dependence of thermal behavior and crystallization behavior.

CRediT authorship contribution statement

Yimin Chen: Writing - original draft. **Rongping Wang:** Conceptualization. **Xiang Shen:** Investigation. **Junqiang Wang:** Formal analysis. **Tiefeng Xu:** .

Declaration of Competing Interest

The authors declare that they have no known competing financial interests or personal relationships that could have appeared to influence the work reported in this paper.

Acknowledgments

The Project is supported by the Natural Science Foundation of China (Grant Nos. 61775111, 61775109, 61904091, and 51771216), Zhejiang Provincial Natural Science Foundation of China (LR18E010002), the Natural Science Foundation of Ningbo City, China (Grant No. 2019A610065), the International Cooperation Project of Ningbo City (Grant No. 2017D10009), One Hundred Talents Program of Chinese Academy of Sciences, 3315 Innovation Team in Ningbo City, and sponsored by K. C. Wong Magna Fund in Ningbo University, China.

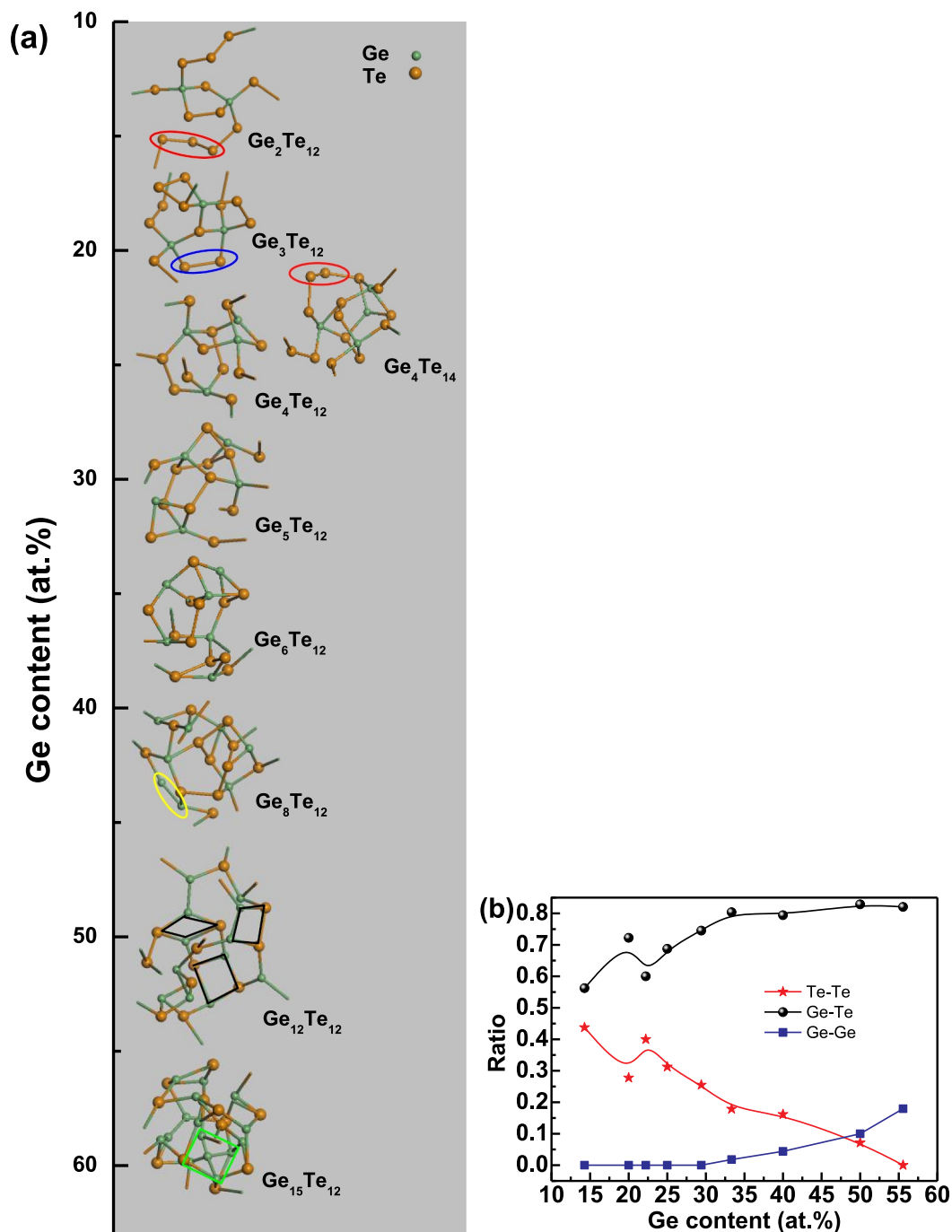


Fig. 6. Component dependences of (a) structural sketch, (b) ratio of bond amount of Te–Te, Ge–Te, and Ge–Ge. The red cycles, blue cycle, yellow cycle, black quadrilaterals and green square in (a) indicate the Te chains, Te–Te bond, Ge–Ge bond, four-atomic ring structures, and GeTe₄ tetrahedron, respectively. The lines in (b) are guides for eye. (For interpretation of the references to color in this figure legend, the reader is referred to the web version of this article.)

References

- [1] M. Micoulaut, Y. Yue, Material functionalities from molecular rigidity, Maxwell's modern legacy, *MRS Bull.* 41 (1) (2017) 18–22.
- [2] Y. Chen, G. Wang, L. Song, X. Shen, J. Wang, J. Huo, R. Wang, T. Xu, S. Dai, Q. Nie, Unraveling the crystallization kinetics of supercooled liquid GeTe by ultrafast calorimetry, *Cryst. Growth Des.* 17 (7) (2017) 3687–3693.
- [3] V. Mittal, A. Aghajani, L.G. Carpenter, J.C. Gates, J. Butement, P.G. Smith, J.S. Wilkinson, G.S. Murugan, Fabrication and characterization of high-contrast mid-infrared GeTe₄ channel waveguides, *Opt. Lett.* 40 (9) (2015) 2016–2019.
- [4] M. Chen, K.A. Rubin, R.W. Barton, Compound materials for reversible, phase-change optical data storage, *Appl. Phys. Lett.* 49 (9) (1986) 502–504.
- [5] Y. Saito, Y. Sutou, J. Koike, Electrical resistance and structural changes on crystallization process of amorphous Ge–Te thin films, *Mater. Res. Soc. Symp. Proc.* 1160 (H12) (2009) 05–10.
- [6] E. Gourvest, S. Lhostis, J. Kreisel, M. Armand, S. Maitrejean, A. Roule, C. Vallée, Evidence of Germanium precipitation in phase-change Ge_{1-x}Te_x thin films by Raman scattering, *Appl. Phys. Lett.* 95 (3) (2009) 031908–031910.
- [7] T. Gwon, A.Y. Mohamed, C. Yoo, E.S. Park, S. Kim, S. Yoo, H.K. Lee, D.Y. Cho, C.S. Hwang, Structural Analyses of Phase Stability in Amorphous and Partially Crystallized Ge-Rich GeTe Films Prepared by Atomic Layer Deposition, *ACS Appl. Mater. Interfaces* 9 (47) (2017) 41387–41396.
- [8] I. Kaban, E. Dost, W. Hoyer, Thermodynamic and structural investigations of heat-

- treated amorphous Ge-Te alloys, *J. Alloy. Compd.* 379 (1–2) (2004) 166–170.
- [9] R. Svoboda, D. Brandová, J. Málek, Non-isothermal crystallization kinetics of GeTe₄ infrared glass, *J. Therm. Anal. Calorim.* 123 (1) (2015) 195–204.
- [10] S. Raoux, B. Muñoz, H.-Y. Cheng, J.L. Jordan-Sweet, Phase transitions in Ge-Te phase change materials studied by time-resolved x-ray diffraction, *Appl. Phys. Lett.* 95 (14) (2009) 143118–143120.
- [11] W. Hoyer, I. Kaban, P. Jónvári, E. Dost, Crystallization behavior and structure of amorphous Ge₁₅Te₈₅ and Ge₂₀Te₈₀ alloys, *J. Non-Cryst. Solids* 338–340 (2004) 565–568.
- [12] N. Yan, X.Q. Liu, L. Zhang, Z. Zhang, X.D. Han, The amount of Ge tunes the atomic structure of amorphous Ge_xTe_{1-x} alloy, *Chem. Phys. Lett.* 556 (2013) 108–112.
- [13] M.N.T. Okabe, Crystallization behavior and local order of amorphous Ge_xTe_{1-x} films, *J. Non-Cryst. Solids* 88 (2–3) (1986) 182–195.
- [14] A.V. Kolobov, P. Fons, A.I. Frenkel, A.L. Ankudinov, J. Tominaga, T. Uruga, Understanding the phase-change mechanism of rewritable optical media, *Nat. Mater.* 3 (10) (2004) 703–708.
- [15] S. Kohara, K. Kato, S. Kimura, H. Tanaka, T. Usuki, K. Suzuya, H. Tanaka, Y. Moritomo, T. Matsunaga, N. Yamada, Y. Tanaka, H. Suematsu, M. Takata, Structural basis for the fast phase change of Ge₂Sb₂Te₅: ring statistics analogy between the crystal and amorphous states, *Appl. Phys. Lett.* 89 (20) (2006) 201910–201912.
- [16] J. Akola, R.O. Jones, Structural phase transitions on the nanoscale: The crucial pattern in the phase-change materials Ge₂Sb₂Te₅ and GeTe, *Phys. Rev. B* 76 (23) (2007) 235201–235210.
- [17] A.B.F. Betts, D.T. Keating, J.P. de Neufville, Neutron and X-ray diffraction radial distribution studies of amorphous Ge_{0.17}Te_{0.83}, *J. Non-Cryst. Solids* 7 (4) (1972) 417–432.
- [18] J.C. Phillips, Topology of covalent non-crystalline solids I: Short-range order in chalcogenide alloys, *J. Non-Cryst. Solids* 34 (2) (1979) 153–181.
- [19] P. Jónvári, I. Kaban, W. Hoyer, R.G. Delaplane, A. Wannberg, Local atomic environment in amorphous Ge₁₅Te₈₅, *J. Phys-Condens. Mater.* 17 (10) (2005) 1529–1536.
- [20] A. Menelle, R. Bellissent, A. Flank, A neutron scattering study of supercooled liquid tellurium, *Europhys. Lett.* 4 (6) (1987) 705–708.
- [21] M. Micoulaut, K. Gunasekera, S. Ravindren, P. Boolchand, Quantitative measure of tetrahedral-sp³ geometries in amorphous phase-change alloys, *Phys. Rev. B* 90 (9) (2014) 094207–094215.
- [22] P. Jónvári, A. Piarristeguy, R. Escalier, I. Kaban, J. Bednarcik, A. Pradel, Short range order and stability of amorphous Ge_xTe_{100-x} alloys (12 ≤ x ≤ 44.6), *J. Phys-Condens. Mater.* 25 (19) (2013) 195401–195409.
- [23] H. Okamoto, Ge-Te (germanium-tellurium), *J. Phase Equilib.* 21 (5) (2000) 496.
- [24] H.E. Kissinger, Reaction kinetics in differential thermal analysis, *Anal. Chem.* 29 (11) (1957) 1702–1706.
- [25] K.S. Andrikopoulos, S.N. Yannopoulos, G.A. Voyiatzis, A.V. Kolobov, M. Ribes, J. Tominaga, Raman scattering study of the a-GeTe structure and possible mechanism for the amorphous to crystal transition, *J. Phys-Condens. Mater.* 18 (3) (2006) 965–979.